

How Aromatic Are Large $(4n + 2)\pi$
Annulenes?

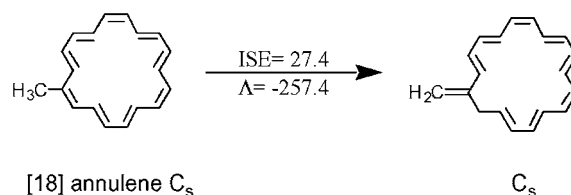
Chaitanya S. Wannere and Paul von Ragué Schleyer*

Computational Chemistry Annex, Department of Chemistry, University of Georgia,
Athens, Georgia 30602-2525

schleyer@chem.uga.edu

Received December 30, 2002

ABSTRACT



While the total aromatic stabilization energies (ASE) of the $[n]$ annulenes, from C_6H_6 to $C_{66}H_{66}$, converge to ca. 22 kcal/mol, the ASEs per π -electron decrease markedly. Bond length alternation (which depends on the theoretical level) only reduces stabilization somewhat but influences the magnetic properties (NICS, proton chemical shifts, and magnetic susceptibilities) considerably. Nevertheless, these magnetic criteria, when based on the most realistic structures, agree that the aromaticities of the larger annulenes decrease and then nearly vanish.

The theory¹ of bonding in cyclic fully conjugated polyenes (annulenes)² predicts “delocalized” structures (highly symmetrical) for the smaller aromatic $[n]$ annulenes but “localized” structures with bond-alternating geometries for higher homologues. Shaik has developed the view that the π -interactions in benzene favor bond alternation, but the σ -framework imposes D_{6h} symmetry.³ While the bond length alternation in higher $(4n + 2)\pi$ -electron $[n]$ annulenes should set in beyond a certain size,⁴ the critical value of “ n ” has still not been established with certainty.⁵ Computational methods including electron correlation favor more sym-

metrical geometries, but the results vary. Using the semiempirical MNDOC method, Yoshizawa found [30]annulene to prefer a bond-alternating D_{3h} geometry over the D_{6h} structure by 4.6 kcal/mol.⁶ However, Choi and Kertesz (CK) reported that this energy difference was only 0.1 kcal/mol at B3LYP/6-31G*.⁷ Bond-alternating forms generally became progressively more stable in higher $[n]$ annulenes (for example, $n = 42, 54,$ and 66).

Resonance energy⁸ estimations for [18]annulene have ranged from Dewar’s⁹ 2.9 kcal/mol to an “experimental value” (based on an energy comparison with benzene) of 100 kcal/mol!¹⁰ Both Siegel and Baldrige¹¹ as well as CK^{7a} evaluated a RE ca. 18 kcal/mol, by comparing [18]annulene with hexatriene and butadiene. However, this procedure is unsatisfactory since the reference molecules do not mimic the HH repulsions and other strain effects in the constricted

(1) (a) Hückel, E. *Z. Phys.* **1931**, *70*, 204. (b) Longuet-Higgins, H. C.; Salem, L. *Proc. R. Soc.* **1959**, *251*, 172. (c) Coulson, C. A.; Dixon, W. T. *Tetrahedron* **1962**, *17*, 215.

(2) (a) Minkin, V. I.; Glukhovtsev, M. N.; Simkin, B. Y. *Aromaticity and Antiaromaticity. Electronic and Structural Aspects*; Wiley & Sons: New York, 1994. (b) Balaban, A. T.; Banciu, M.; Ciorba, V. *Annulenes, Benzo-Hetero-, Homo-Derivatives, and Their Valence Isomers*; CRC Press: Boca Raton, Florida, 1986.

(3) (a) Hiberty, P. C.; Danovich, D.; Shurki, A.; Shaik, S. *J. Am. Chem. Soc.* **1995**, *117*, 7760. (b) Haas, Y.; Zilberg, S. *J. Am. Chem. Soc.* **1995**, *117*, 5387. (c) Shaik, S.; Shurki, A.; Danovich, D.; Hiberty, P. C. *J. Am. Chem. Soc.* **1996**, *118*, 666.

(4) (a) Kuhn, H. *J. Chem. Phys.* **1948**, *16*, 840. (b) Dewar, M. J. S. *J. Chem. Soc.* **1952**, 3544. (c) Labhart, H. *J. Chem. Phys.* **1957**, *27*, 957. (d) Ooshika, Y. *J. Phys. Soc. Jpn.* **1957**, *12*, 1246. (e) Haddon, R. C. *J. Am. Chem. Soc.* **1979**, *101*, 1722.

(5) We will address this problem in a separate paper. See refs 6 and 7 for recent discussions.

(6) Yoshizawa, K.; Kato, T.; Yamabe, T. *J. Phys. Chem.* **1996**, *100*, 5697.

(7) (a) Choi, C. H.; Kertesz, M. *J. Chem. Phys.* **1998**, *108*, 6681. (b) Choi, C. H.; Kertesz, M. *J. Am. Chem. Soc.* **1997**, *119*, 11994.

(8) Pauling, L.; Sherman, J. *J. Chem. Phys.* **1933**, *1*, 606.

(9) Dewar, M. J. S.; Llano, C. *J. Am. Chem. Soc.* **1969**, *91*, 789.

(10) (a) Beezer, A. E.; Mortimer, C. T.; Springall, H. D.; Sondheimer, F.; Wolovsky, R. *J. Chem. Soc.* **1965**, 216. (b) For recent discussions, see also: Oth, J. F. M.; Gilles, J.-M. *J. Phys. Chem. A* **2000**, *104*, 7980.

(11) Baldrige, K. K.; Siegel, J. S. *Angew. Chem., Int. Ed. Engl.* **1997**, *36*, 745.

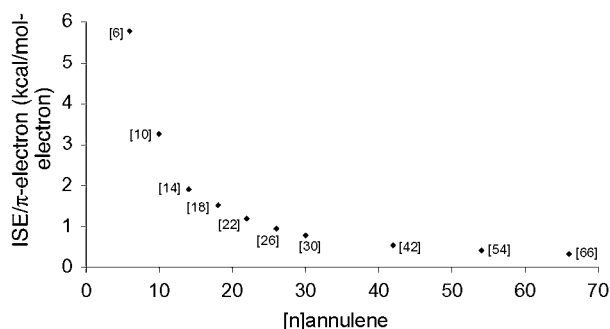


Figure 1. ISE per π -electron, computed using Scheme 1 (at B3LYP/B3LYP), versus the ring size for annulenes.

annulene geometry. Employing the energies of molecular fragments based on the optimized geometries of [18]-annulenes, CK obtained 39.1 kcal/mol^{7a} but considered this ASE to be too high. However, the same fragment method appeared to give reliable ASE results for the larger, less strained annulenes, which approached a constant value near 23 kcal/mol. CK also reported NICS¹² for the [14]-, [18]-, [22]-, [26]-, [30]-, [42]-, [54]-, and [66]annulenes.^{7a} We have now improved and augmented their results significantly.

Our isomerization stabilization energy (ISE) method¹³ evaluates ASEs¹⁴ consistently and reliably for the whole set of strained and unstrained annulenes (see Figure 1). Both HF (bond-alternating) and B3LYP (bond-equalized) geometries have been employed for energy and magnetic property evaluations. Even though ISEs are almost the same for both sets of structures, NICS, proton chemical shifts, and magnetic susceptibility exaltations, Λ ,¹⁵ are very sensitive to the geometries.

Geometries and Energies. All the [n]annulenes ($n \geq 10$) favor bond-alternating structures at HF//HF (Table 1). In contrast, lower energy bond-alternating minima are found

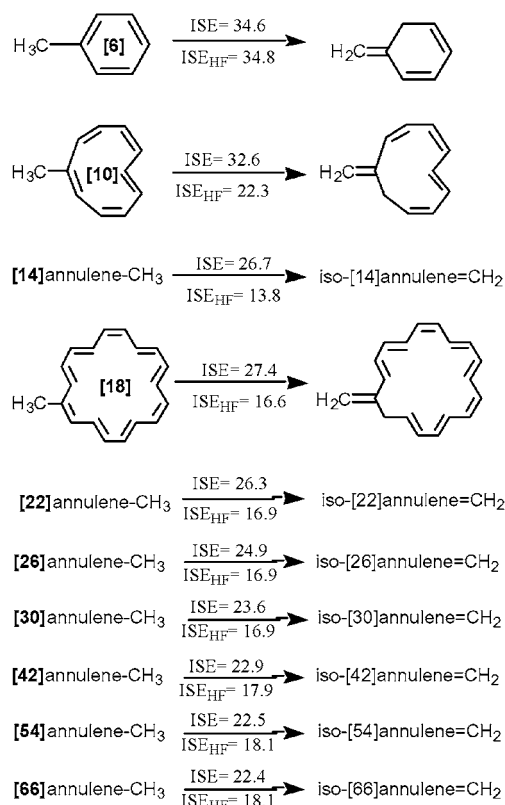
(12) (a) Schleyer, P. v. R.; Maerker, C.; Dransfeld, A.; Jiao, H.; Hommes, N. J. R. v. E. *J. Am. Chem. Soc.* **1996**, *118*, 6317. (b) Schleyer, P. v. R.; Jiao, H.; Hommes, N. J. R. v. E.; Malkin, V. G.; Malkina, O. L. *J. Am. Chem. Soc.* **1997**, *119*, 12669. (c) Schleyer, P. v. R.; Manoharan, M.; Wang, Z. X.; Kiran, B.; Jiao, H.; Puchta, R.; Hommes, N. J. R. v. E. *Org. Lett.* **2001**, *3*, 2465.

(13) Schleyer, P. v. R.; Pühlhofer, F. *Org. Lett.* **2002**, *4*, 2873. The ISE method compares the computed energy of a methyl derivative of a given aromatic system with its structurally closely related nonaromatic exocyclic methylene isomer. See Scheme 1. ISEs were computed at three different levels: HF/6-31G**/HF/6-31G*, B3LYP/6-31G**/HF/6-31G*, and B3LYP/6-31G**/B3LYP/6-31G* designated as HF/HF, B3LYP/HF, and B3LYP/B3LYP, respectively, in subsequent text.

(14) Geometry optimizations, energy evaluations (with ZPE corrections), and frequency analyses, of all the structures in Scheme 1 and in Table 1, were carried out first at HF/6-31G* and then at B3LYP/6-31G*, using Gaussian 98 (reference in Supporting Information). Planar conformations of methyl annulenes and their respective nonaromatic isomers were forced, in order to compute the ISEs and Λ , since the ISEs using their nonplanar analogues were not different (e.g., ISE of 22.2 for nonplanar vs 27.4 kcal/mol for planar methyl[18]annulene at B3LYP/6-31G*).

(15) (a) Dauben, H. J.; Wilson, J. D.; Laity, J. L. *Nonbenzenoid Aromaticity*; Snyder, J. P., Ed.; Academic Press: New York, 1971; Vol. II, and references therein. (b) Jiao, H.; Schleyer, P. v. R. *Angew. Chem., Int. Ed. Engl.* **1993**, *32*, 1763. (c) Herges, R.; Jiao, H.; Schleyer, P. v. R. *Angew. Chem., Int. Ed. Engl.* **1994**, *33*, 1376. (d) Schleyer, P. v. R.; Jiao, H. *Pure Appl. Chem.* **1996**, *68*, 209.

Scheme 1. ISE and ISE_{HF} (in kcal/mol, ZPE corrected) at B3LYP/6-31G**/B3LYP/6-31G* and HF/6-31G**/HF/6-31G* energies, respectively^a



^a C_s geometries were used.

only for the higher [n]annulenes ($n \geq 30$) at B3LYP//B3LYP.¹⁶ In these annulenes, the D_{6h} forms were obtained by imposing symmetry.

Notably, these D_{6h} forms were only between 0.26 [$n = 30$] and 6.1 kcal/mol [$n = 66$] higher in energy than the D_{3h} minima (E_{rel} , Table 1). In contrast, the B3LYP//HF single-point relative energies (Table 1) increased steadily from 2.92 [$n = 10$] to 28.33 kcal/mol [$n = 66$]. However, this increase was not due solely to the decrease in resonance energy in bond-localized geometries. Geometrical parameters at HF are not optimal for B3LYP energy evaluations.

The ISE evaluations are more instructive. The ISEs of many of the annulenes at HF//HF (Scheme 1) and of all the annulenes at B3LYP//HF (Table 1) are only slightly smaller than those evaluated at B3LYP//B3LYP. The deviations, the ISE data at HF//HF, start at [$n = 10$] but then become progressively smaller as n increases (Scheme 1). Notably, the ISEs of large annulenes approach plateaus of 18 (HF//HF) and 22 kcal/mol (B3LYP//B3LYP) (Scheme 1). These plateaus, which match CK's,^{7a} are much larger than Dewar's predicted ca. 2.8 kcal/mol. However, the ISE per π -electron, a more important measure of aromaticity of such different systems, decreases markedly with increasing annulene ring size (Figure 1).

(16) At B3LYP//B3LYP, a slight C–C bond alternation, 0.04 Å, sets in at [30]annulene.

Table 1. Relative Energies (E_{rel} , kcal/mol), Total NICS(0) and Dissected π -Contributions (at the ring centers), Magnetic Susceptibility Exaltations (Λ , cgs ppm), and Averaged Inner and Outer ^1H NMR Chemical Shifts of the $[n]$ Annulenes^a

$[n]$	method/6-31G*	E_{rel}^b	ISE ^c	NICS(0) ^d	NICS(π) ^d	$\Lambda^e(\Lambda^f)$	$\delta H_{\text{inner}}^d$	$\delta H_{\text{outer}}^d$
[6]	D_{3h} B3LYP//HF	4.50 ^g		-8.3	-20.1	-17.0		7.5
	D_{6h} B3LYP//B3LYP	0.00	(34.6)	-8.8	-20.7	-17.6 (-15.8)		7.5
[10]	C_s B3LYP//HF	2.92	(31.1)	-28.8	-17.7	-52.4 (-54.0)	-5.7	8.4
	C_{2v} B3LYP//B3LYP	0.00	(32.6)	-28.6	-17.7	-54.8 (-64.2)	-5.9	8.7
[14]	C_{2v} B3LYP//HF	10.39	(20.9)	-7.5	-10.7	-71.2 (-79.9)	-1.8	8.5
	D_{2h} B3LYP//B3LYP	0.00	(26.7)	-13.4	-15.7	-118.0 (137.3)	-7.5	10.1
[18]	D_{3h} B3LYP//HF	12.03	(21.9)	-5.9	-8.4	-99.0 (-105.9)	-1.6	8.8
	D_{6h} B3LYP//B3LYP	0.00	(27.4)	-15.9	-15.9	-232.7 (-257.4)	-11.2	11.8
[22]	C_{2v} B3LYP//HF	13.12	(21.2)	-4.9	-6.8	-113.9 (-122.1)	-0.8	8.8
	D_{2h} B3LYP//B3LYP	0.00	(26.3)	-15.2	-16.2	-390.3 (-416.7)	-14.1	13.3
[26]	C_{2v} B3LYP//HF	13.87	(20.5)	-3.9	-5.0	-123.3 (-131.4)	0.1	8.7
	D_{2h} B3LYP//B3LYP	0.00	(24.9)	-15.8	-16.1	-631.7 (-599.1)	-17.0	15.2
[30]	D_{3h} B3LYP//HF	14.78	(20.1)	-3.0	-3.9	-125.7 (-133.2)	1.1	8.5
	D_{3h} B3LYP//B3LYP	0.00	(23.6)	-13.8	-14.4	-755.4 (-741.2)	-16.1	15.6
	D_{6h} B3LYP//B3LYP	0.26		-16.2	-16.5	-978.0	-20.0	17.2
[42]	D_{3h} B3LYP//HF	18.61	(20.7)	-1.1		-89.3 (-89.3)	3.6	7.7
	D_{3h} B3LYP//B3LYP	0.00	(22.9)	-5.6		-916.6 (-940.9)	-6.5	10.8
	D_{6h} B3LYP//B3LYP	1.88		-16.7		-2636.2	-28.8	21.7
[54]	D_{3h} B3LYP//HF	23.32	(20.8)	0.0		-51.8 (-46.7)	4.8	4.9
	D_{3h} B3LYP//B3LYP	0.00	(22.5)	-2.6		-893.9 (-900.0)	-1.3	8.7
	D_{6h} B3LYP//B3LYP	3.84		-17.0		-5564.8	-37.2	28.0
[66]	D_{3h} B3LYP//HF	28.33	(20.8)	0.1		-30.0 (-21.1)	5.0	4.8
	D_{3h} B3LYP//B3LYP	0.00	(22.4)	-1.2		-758.3 (-760.3)	1.7	7.2
	D_{6h} B3LYP//B3LYP	6.10		-17.1		-10125.0	-45.0	34.5

^a Values in parentheses are the isomerization stabilization energies (ISE, kcal/mol) and magnetic susceptibility exaltations (Λ , cgs ppm), evaluated using the $[n]$ annulene derivatives in Scheme 1. ^b Computed at B3LYP/6-31G*//. ^c Evaluated at B3LYP/6-31G*// + ZPE (at the same level) for $n < 30$ and without ZPE correction for $n \geq 30$. ^d NICS(0), NICS(π), H_{outer} , and H_{inner} at IGLO/TZ2P// for $n \geq 30$ and at GIAO-B3LYP/6-31G*// for $n > 30$. ^e $\Lambda = \chi_{\text{M}} - \chi'_{\text{M}}$. Magnetic susceptibilities of aromatic annulenes, χ_{M} , at CSGT-B3LYP/6-31+G*// (for $n \geq 30$) and at CSGT-B3LYP/6-31G*// (for $n > 30$); magnetic susceptibilities of nonaromatic annulenes, χ'_{M} evaluated by using increments (see ref 21). ^f Λ based on Scheme 1 at CSGT-B3LYP/6-31+G*// for $n \geq 30$ and at CSGT-B3LYP/6-31G*// for $n > 30$. ^g With fixed 1.449 and 1.350 Å C–C bond lengths.

Note that the HF//HF ISEs (Scheme 1) are almost as large as those at B3LYP//B3LYP, despite the differing preferences for bond-alternating geometries, $[n > 6]$ at HF//HF and $[n \geq 30]$ at B3LYP//B3LYP. Consequently, “bond localization” in these B3LYP-optimized large annulenes *does not* result in a major loss of stabilization energy. The same conclusion has been reached for benzene, after imposition of Kekulé cyclohexatriene geometries (Table 1).^{12a,b,17}

The computed B3LYP ISEs of [18]annulene, 27.4 kcal/mol on the more regular //B3LYP structures and 21.9 kcal/mol on the //HF geometries (Table 1), lie between CK’s two ASE estimates, 16.4 and 39.1 kcal/mol. Although our B3LYP//B3LYP ISEs for [42]-, [54]-, and [66]annulenes (22.9, 22.5, and 22.4 kcal/mol, respectively, Table 1) are in remarkably good agreement¹⁸ with CK’s B3LYP values (23.2, 22.6 and 23.1 kcal/mol, respectively). Because of the close relationship of the structures involved, the ISE method deals with strained molecules more effectively.¹⁴

Magnetic Properties. Arguably, magnetic criteria (Λ ,¹⁹ ^1H NMR chemical shifts,²⁰ as well as NICS and its dissection into π -contributions) provide the best measures of aromaticity

since they are based directly on the special “ring current” effects due to cyclic electron delocalization. More than the energies, the magnetic properties are influenced by the geometries dramatically (see Table 1).

Magnetic susceptibility exaltations, Λ , are closely associated with aromaticity.¹³ Evaluations ($\Lambda = \chi_{\text{M}} - \chi'_{\text{M}}$) are based on the magnetic susceptibilities of an annulene (χ_{M}) and its nonaromatic model (χ'_{M}). The annulene Λ values computed via the ISE equations of Scheme 1¹⁹ (values in parentheses in Table 1) agree well with those using increments.²¹ Due to the greater ring area, Λ s for the large B3LYP-optimized annulenes are much greater than those for the small annulenes. The ring current contribution to the total χ of a cyclic compound is proportional to the product of the square of the ring area (θ^2) and ASE.^{2a,22} Indeed, we find that Λ follows this expectation, but only for $[n \leq 30]$. The curve falls off for D_{3h} [42]-, [54]-, and [66]annulenes (see Figure A in Supporting Information), but the much larger

(19) Λ evaluated at CSGT-B3LYP/6-31+G*//B3LYP/6-31+G**.

(20) NICS and ^1H NMR chemical shift employed the PW-91 functional, the IGLO-III TZ2P basis set, and the Pipek–Mezey σ,π -localization available in the deMon NMR program.

(21) Our increment scheme was based on magnetic susceptibilities of ethylene and butadiene. The $\text{CH}_2=$ and $=\text{CH}-$ increments are -7.3 and -5.1 cgs ppm, respectively.

(22) Maoche, B.; Gayoso, J.; Ouamerli, O. *Rev. Roum. Chem.* **1984**, *29*, 613.

(17) Fleischer, U.; Kutzelnigg, W.; Lazzeretti, P.; Mühlenkamp, V. *J. Am. Chem. Soc.* **1994**, *116*, 5298.

(18) When applied to the HF//HF geometries, CK’s procedure gives ASEs [see Supporting Information] in gross disagreement with our ISEs. CK did not evaluate the ASEs of [10]-, [14]-, [22]-, and [26]annulenes.

Λ s for their D_{6h} forms (e.g., $-10\ 125$ for [66]annulene!) continue the initial trend.

The computed proton chemical shifts also are extremely sensitive to the geometry. As is well-known,^{2a} the δ ^1H s of the inner and the outer annulene protons can differ dramatically (Table 1) from those of normal alkenes ($\delta = 5.6$ for cyclohexene). The outer Hs are downfield (also from benzene, $\delta = 7.2$), but the inner Hs are upfield, evidently due to the strong diatropic ring currents in these annulenes. The δ ^1H s computed on the most symmetrical B3LYP geometries (Table 1) increase steadily to very large negative (H_{inner}) and positive (H_{outer}) values, but these are far away from the experimental^{2a} δ ^1H s. The HF geometries also do not give reliable δ ^1H s either.

The behavior of the computed δ ^1H s using the bond-localized HF-optimized annulene geometries is quite different. The inner–outer δ ^1H difference is the largest for [$n = 10$] but then decreases with increasing ring size, slowly at first and then rapidly to the vanishing point. There is no δ ^1H difference between the olefin-like outer and the inner proton chemical shifts for [54]- and [66]annulenes using the D_{3h} HF geometries. The less bond length-alternating B3LYP-optimized D_{3h} [$n > 30$]annulene geometries (details in Supporting Information) result in intermediate behavior: the inner–outer δ ^1H differences decrease steadily with ring size.

The NICS values (Table 1) also depend markedly on the geometry for [$n > 10$]. Understandably, NICS(0) in the annulene centers (as well as its dissected π -contribution, NICS(π)) mirrors the behavior of the inner proton chemical shifts: the magnitudes are largest for the D_{6h} geometries (where they reach a constant value of about -17), smaller for the //B3LYP D_{3h} minima, and smallest to negligible for the //HF geometries.

The NICS(0) values for the D_{3h} B3LYP and especially the HF-optimized minima decrease rather rapidly with increasing size. This follows the ISE/ π -electron behavior of Figure 1 and also the Λ and δ ^1H trends. However, Λ , ISE, and δ ^1H , but *not* NICS(0), predict that the B3LYP-optimized D_{3h} “bond-alternating” structure of [66]annulene retains “significant aromatic character”. The HF-optimized bond-alternating [54]- and [66]annulenes have small ISE/ π -electron values, Λ s, δ ^1H NMR differences, and NICS (Table 1); evidently these annulenes behave more like cyclized long-chain polyenes.

We conclude that the best interpretations of the criteria investigated all establish the decrease in aromaticity along the [n]annulene series. The trend toward greater bond alternation increases with ring size; its onset occurs at [$n = 10$] at HF/6-31G* but at [$n = 30$] at B3LYP/6-31G*. However, this DFT level may favor the higher symmetry annulene structures excessively.²³ The ISE method gives consistent and evidently reliable energies, particularly for the strained systems where other ASE evaluations are problematic. The ISE per π -electron decreases to very small values with increasing ring size (Figure 1). The Λ , NICS, and ^1H NMR chemical shifts depend markedly on the annulene geometries, but the more realistic lower-symmetry structures also follow the trend toward smaller aromaticity. The HF D_{3h} forms of the largest annulenes show nonaromatic δ ^1H behavior; also, their ISE/electron, Λ , and NICS values are quite small.

The ISE differences, based on bond-equalized (B3LYP) and bond-localized (HF) optimized structures, are small. In contrast, the magnetic criteria are very sensitive to the geometries. Neither B3LYP nor HF geometries give computed proton chemical shifts in agreement with experiment. We intend, in the future, to employ this sensitivity, along with experimental data comparisons, to establish the reliability of structures computed at various theoretical levels.

Acknowledgment. We thank Norman L. Allinger for helpful discussions. The University of Georgia and National Science Foundation Grant CHE-0209857 provided financial support.

Supporting Information Available: Detailed computational output information for all of the structures in Scheme 1 and Table 1, as well as Figure A demonstrating that Λ is proportional to the product of θ^2 and ISE for [$n \geq 30$]annulenes. This material is available free of charge via the Internet at <http://pubs.acs.org>.

OL027571B

(23) King, R. A.; Crawford, D.; Stanton, J. F.; Schaefer, H. F. *J. Am. Chem. Soc.* **1999**, *121*, 10788.